Simulation Study of Dipole-Induced Self-Assembly of Nanocubes

Xi Zhang,[†] Zhenli Zhang,[‡] and Sharon C. Glotzer*[,†,‡]

Department of Materials Science and Engineering and Department of Chemical Engineering, University of Michigan, Ann Arbor, Michigan, 48109-2136

Received: September 12, 2006; In Final Form: December 30, 2006

Recent experiments have demonstrated that nanoparticles with dipoles can self-assemble into interesting one-dimensional and two-dimensional nanostructures. In particular, nanocubes with dipoles are found to form straight nanowires and nanorings with potential applications for nanodevices. In this paper, we use a minimal model to study dipole-induced self-assembly of nanocubes with varying dipole directions, dipole strengths and both with and without face−face attractions arising from dispersive or solvophobic interactions. We reproduce the structures observed in experiments and illustrate that the self-assembled morphologies are dictated by the head-to-tail alignment of the dipoles, the orientation of the dipoles within the cubes, and the face-to-face packing of the nanocubes. Our results show how the self-assembly of dipolar nanocubes differs from that of dipolar spheres in which the only anisotropy is the dipole itself and how system parameters can be manipulated to control the assembled morphologies and the phase behavior. Our simulation model, which uses the plane separating algorithm for efficient detection of nanoparticle overlaps, can be utilized to investigate the self-assembly of other smooth, convex polyhedral-shaped nanoparticles to facilitate novel nanomaterials design.

1. Introduction

Self-assembly of nanoscale molecules and particles into tailored nanostructures with enhanced properties and novel applications is a promising strategy for "bottom-up" materials design.[1] As the first step, nanoparticles with a wide variety of shapes, including rods, wires, rings, cubes, tetrapods, triangular prisms, and many other exotic shapes[2] have been synthesized. The next step, organizing these nanoparticles into predefined, specific structures exhibiting desired properties, is a formidable challenge now facing the materials community. When nanoparticles aggregate, they often form simple two-dimensional (2D) and three-dimensional (3D) arrays or "superlattices".[3,4] In many cases, the different nanoparticle shapes only affect the particle arrangement within these arrays and not the final, overall structures.[4] In particular, most nanocubes are observed to form 2D square arrays.[4]

Introducing directional, anisotropic interactions from magnetic[5] or electric dipoles[6] is a practical strategy to impart anisotropy into self-assembled morphologies. For example, Kotov and co-workers have demonstrated that CdTe nanoparticles self-assemble into chains due to the strong electronic dipole−dipole attractions between the nanoparticle cores.[7,8] Silver nanocrystals are also observed to form chains,[9] possibly due to the attractions between magnetic dipoles. Recently, Cho et al. discovered nanowires as well as nanorings resulting from the dipole-induced orientational attachment of cubic PbSe nanoparticles.[10] These assembled nanostructures have interesting optical, magnetic, and electronic properties, and hold tremendous potential for applications in electronic and photonic devices, telecommunications, and sensors.[6]

Computer simulations have played an important role in understanding the structures and phase behavior of fluids of dipolar particles.[11] Weis and Levesque performed Monte Carlo (MC) simulations of dipolar hard spheres (DHS) and observed linear, chain-like structures formed by the spheres at low densities.[12] Tavares et al.[13] carried out extensive MC simulations on a large number of DHS particles to study the chainlike structures. Their results semiquantitatively agree with the prediction of living polymerization theory. Stevens and Grest studied dipolar soft spheres (DSS) and also discovered chainlike structures in their MC simulations.[14] These chainlike structures are the consequence of head-to-tail alignment of dipoles, which is the energy minimum for dipole−dipole interactions.[15] An interesting feature of DHS and DSS phase behaviors is the lack of a liquid−vapor critical point. Simulations suggest that the "conventional" phase behavior can be recovered by stretching spheres into rods[16] or adding attractive van der Waals interactions between particles.[17] There is also a wealth of theoretical and simulation work on the structures and phase diagrams of dipolar rods.[18,19] It is found that the side-by-side packing of dipoles stabilizes liquid crystal phases (including nematic and smectic phases), and leads to the formation of ferroelectric phases.

Although it is well established in the dipolar fluid and liquid crystal communities that the alignment of dipoles dictates the self-assembly of dipolar spheres and rods[18,19] the effect of dipolar interactions on the self-assembly of polyhedral nanoparticles has received comparatively little study. For example, our recent studies[20] indicated that the self-assembly of dipolar nanotetrahedra are altered by their face-to-face packing. It is of interest to know how nanoparticle shape and dipole interactions combine to contribute to the self-assembly of dipolar nanocubes. In particular, as the dipole can orient in several directions relative to a cube face, interesting packing behavior that differs from

* Corresponding author. Email: sglotzer@umich.edu.
[†] Department of Materials Science and Engineering.
[‡] Department of Chemical Engineering.

10.1021/jp065953j CCC: $37.00
Published on Web 02/23/2007

TABLE 1: Probabilities of Dipole Directions and Strengths in Nanocubes with Random Distribution of Polar Corners

dipole direction	dipole strength ($\mu/\mu_{<100>_a}$)	probability
N/A	0	0.114
$<100>_a$	1	0.343
$<100>_b$	2	0.086
<110>	$\sqrt{2}$	0.343
<111>	$\sqrt{3}$	0.114

that observed with spheres is likely, as demonstrated by the experiments of Cho et al.[10]

Here we perform the first simulation study of dipole-induced self-assembly of attractive nanocubes, inspired by and modeled after the experimental work by Cho et al.[10] We examine the self-assembled structures and phase behavior as a function of varying dipole direction, dipole strength, and both the presence of and strength of face−face attraction. Our simulation results reproduce the self-assembled structures observed in the experiments and provide insight into the assembly processes. We find that the self-assembled morphologies are dictated by the head-to-tail alignment of dipoles coupled with the dipole direction within the cubes and the tendency for face-to-face packing of the nanocubes. We demonstrate that attractive interactions that promote face−face alignment can also be utilized to control the assembled morphologies. Our study suggests new opportunities for the rational design of novel nanomaterials.

Our paper is organized as follows. We describe our model and simulation method in Section 2. In section 3.1, we investigate the effect of nanoparticle shape on self-assembly of cubes with <100> dipoles for varying volume fraction, dipole strength, and cube size in the absence of face-to-face attractive interactions induced by dispersive or solvophobic interactions. In section 3.2, we include face-to-face dispersive or solvophobic attractions and compare with the structures reported in 3.1. In section 3.3, we investigate the effect of nanoparticle shape on self-assembly of cubes with <110> dipoles and compare with the results in 3.1, and in section 3.4 we investigate self-assembly of mixtures of dipoles with different strengths and interactions. We present our conclusions in section 4.

2. Model

Cho et al. conjectured that the electronic dipoles in PbSe nanocubes originate from the noncentrosymmetric arrangement of Pb- and Se-terminated, polar, {111} facets on the cube corners.[10] The dipole moment contribution from a Pb-terminated corner (net charge $+q$) and a Se-terminated corner (net charge $-q$) is, $\vec{p} = q\vec{d}$ in which d is the distance between the two corners. Assuming a random distribution of four Pb-terminated and four Se-terminated corners, we calculate the probabilities of possible dipole moments and list them in Table 1. As shown in Table 1, a majority (77.2%) of nanocubes have either <100> or <110> dipole directions. Therefore, we focus our simulations on these two dipole directions. Figure 1 shows our model cubes with <100> and <110> dipoles fixed at the cube centers. We note that for <100> dipoles there are two possible values of dipole moment magnitude, or dipole strength, with a ratio of 2:1.

The dipole−dipole interactions are calculated using the equation

$$U_{\mathrm{d}} = \frac{\vec{\mu}_i \cdot \vec{\mu}_j}{r_{\mathrm{ij}}^{\,3}} - 3\frac{(\vec{\mu}_i \cdot \vec{r}_{ij})(\vec{\mu}_j \cdot \vec{r}_{ij})}{r_{\mathrm{ij}}^{\,5}}$$

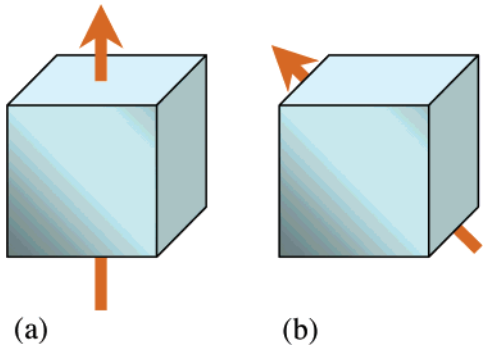

Figure 1. Model systems. (a) Nanocube with <100> dipole. (b) Nanocube with <110> dipole. The arrows represent the dipole directions.

where $\vec{\mu}_i$ is the dipole moment on cube i, and $\vec{r}_{ij}$ is the separation vector between the mass centers of cube i and cube j. The interactions between cube pairs are truncated at half the box length, following the minimum image (MI) convention. We chose not to use the computationally expensive Ewald summation method, as our study is focused on the assembled morphologies at low densities. Previous MC simulations have demonstrated that at low densities, the structures and thermodynamic properties of dipolar fluids exhibit no significant discrepancy between MI and Ewald simulation results.[21−23]

Attractive interactions (such as van der Waals and hydrophobic interactions) promoting face−face cube alignment are modeled with a square-well potential. If two faces of neighboring cubes have face-to-face close packing, judging by the criteria of $d < 0.01$ and $\cos(\theta) < 0.01$ in which d is the distance between the two face centers in units of the cube edge length and θ is the angle between the two face normals, a negative term of $-\epsilon$ is added to the potential energy between the two cubes in which ϵ is the face−face attraction strength.

We perform canonical ensemble MC simulations with the conventional Metropolis algorithm.[24] Each MC step (MCS) in our simulations consists of $0.1N$ displacement trial moves and $0.9N$ rotational trial moves, where N is the number of nanocubes in the system. The rotational trial moves are handled using the method of quaternions.[24] The maximum trial move displacement is adjusted every 10^5 MC steps, aiming for an average trial acceptance ratio around 0.6. We adopt the plane separating algorithm (PSA)[25] to efficiently detect overlaps between nanocubes. Escobedo et al. used the oriented bounding box (OBB) algorithm, a special case of PSA, to simulate cuboids.[26] Here we choose PSA over OBB as PSA can detect the overlaps between all convex polyhedra, while OBB is restricted to cube-like shapes with rectangular bounding boxes.

Each simulation starts from a sufficiently high temperature to ensure a disordered initial configuration. The cooling process is simulated by slowly ($\Delta T < 0.01$) cooling the system to the target temperature, while monitoring the potential energy to ensure equilibrium is reached at each temperature step. The heating process is likewise simulated after the completion of the cooling process. Regarding the parameters chosen for study, we use a similar dipole strength ($\mu = 4$) as used in previous simulation studies of dipolar hard spheres and dipolar soft spheres. With this dipolar strength wires and chains are found for dipolar spheres. We varied the face−face attraction over a range of values and found that $\epsilon = 4$ is a typical value at which the cubes assemble, and $\epsilon = 8$ and 16 are the values at which we observe differences in assembled morphologies. We thus focus on these values to elucidate the various assembled structures.

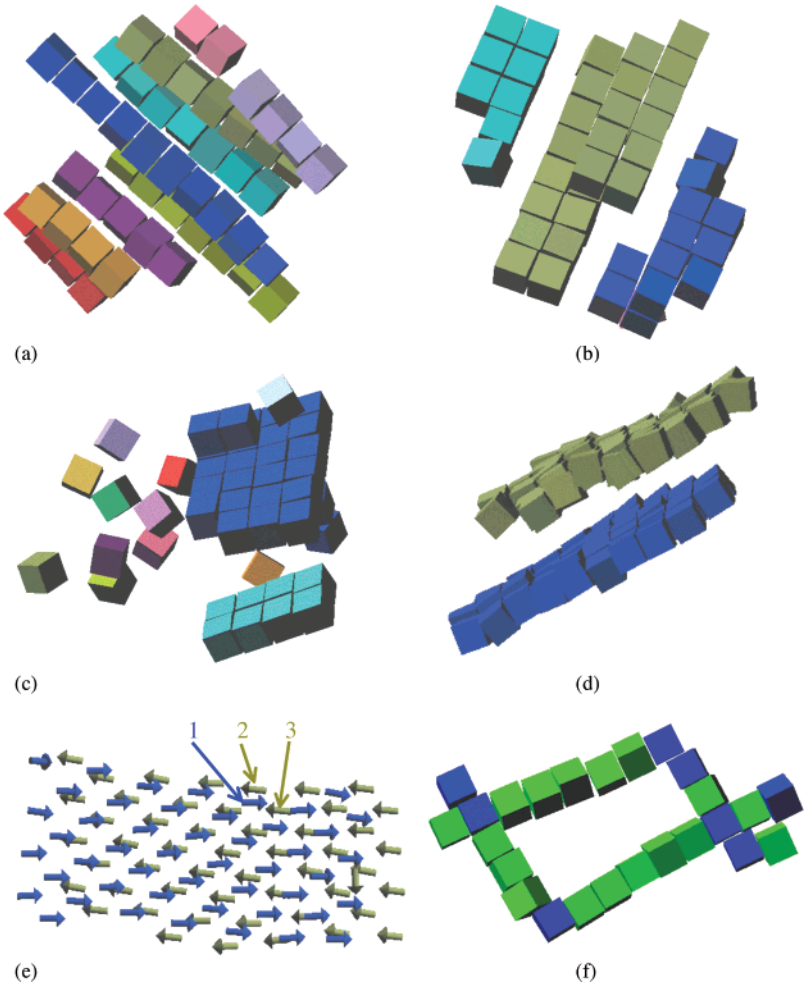

Figure 2. Self-assembled morphologies from simulation snapshots. Cubes within the same mesostructure are colored the same. (a) Nanowires from nanocubes with <100> dipoles. (b) Stacked wires from nanocubes with <100> dipoles and moderate face−face attractions ($\epsilon = 8$). (c) Sheetlike structure from nanocubes with <100> dipoles and strong face−face attractions ($\epsilon = 16$). (d) Sheets from nanocubes with <110> dipoles. (e) Dipole directions in sheets formed by nanocubes with <110> dipoles. (f) Nanoring from nanocubes of mixed dipole directions and strengths (green cubes have <100> dipole of strength $\mu = 4$; blue cubes have <110> dipole of strength $\mu = 5.66$).

Various systems sizes are simulated to eliminate finite size effects on self-assembled morphologies. We find that systems of 20, 50, 100, and 200 nanocubes all result in the same morphologies at the same state points. Therefore, our production runs are performed on systems of 50 cubes to minimize the computational cost of the simulations while still obtaining statistically significant structures. At each temperature step a typical simulation run reaches equilibrium in 30∼1200 million MCS, and then 200∼500 million additional MCS are carried out to collect data. Each simulation takes about 20∼800 h on an Athlon 2400MP processor.

The constant volume heat capacity, C_v, can be calculated from the equation

$$C_v = \frac{1}{k_B T^2}[\langle U^2\rangle - \langle U\rangle^2]$$

where U is the potential energy and T is the temperature. The volume fraction ϕ of the system is defined as $\phi = N\sigma^3/V$, where σ is the edge length of a cube and V is the volume of the simulation box. The reduced temperature T^* is defined as $T^* = k_B T\sigma^3/\mu^2$, following the convention for dipolar fluids.[11]

3. Results and Discussion

3.1. Straight Nanowires Assembled from Nanocubes with <100> Dipoles. First, we simulate nanocubes with <100> dipoles (model shown in Figure 1a) and no face−face attractions. Figure 2a shows the one-dimensional chains (wires) self-assembled on cooling from 50 nanocubes at $\phi = 0.1$ and $T = 0.3$. Dipoles in the assembled nanowires display the same head-to-tail arrangement as in DHS and DSS systems.[15] However, unlike the sphere systems, the cubes do not form curved chains,[12−14] but instead they form straight chains, or wires. This difference is caused by the geometry of the nanocubes. To minimize the interaction energy between two head-to-tail aligned dipoles, the face-to-face packing of nanocubes is preferred to minimize the center-to-center distance, resulting in the straight alignment of nanocubes along the <100> direction. Our simulation snapshot shows the same morphology as in the TEM image from the experiment conducted by Cho et al.,[10] except that the experimentally assembled nanowires have smooth side walls and uniform orientations around the <100> direction. This difference is not surprising, as the dipole interaction in our model does not confer any restriction on the rotational degrees of freedom of the cubes around the aligned <100> direction. The smooth wires in the experiment were obtained after being annealed at 170 °C while the aggregated nanocubes fused together. At this time, our minimal model cannot mimic the fusing process; we expect to address this issue with more detailed models in future work. Nonetheless, we have demonstrated that our minimal dipole model can reproduce morphologies similar to those observed in the experiment and thus

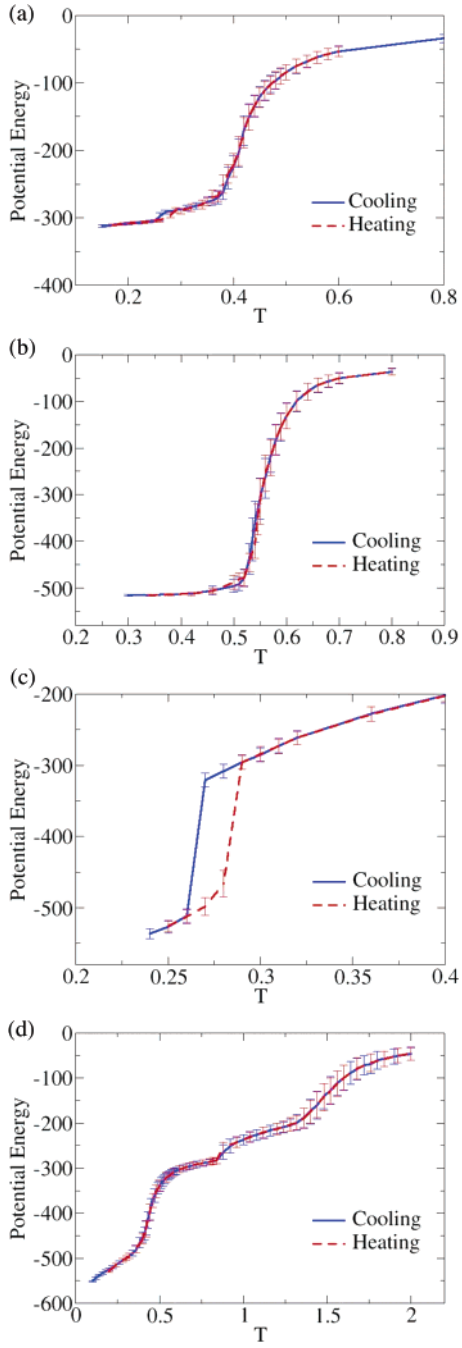

Figure 3. Potential energy vs temperatures plots on cooling and heating for (a) nanocubes with <100> dipoles; (b) nanocubes with <100> dipoles and weak face−face attraction ($\epsilon = 4$); (c) nanocubes with <110> dipoles; (d) nanocubes with <100> dipoles of mixed strengths. The error bars represent the standard deviation in the data calculated over multiple independent runs.

confirm that directional dipole−dipole attractions can drive the self-assembly of nanocubes into straight wires.

With our simulation model, we can further elucidate the thermodynamics of nanocube assembly. Figure 3a shows the potential energy vs temperature plots for both cooling and heating processes. The plots show continuous transitions with no hysteresis, suggesting an "equilibrium polymerization" type of transition.[23] The transition temperature, T_p, can be identified by locating the maximum in constant volume heat capacity vs temperature plots.[23] The analogy between self-assembly of dipolar spheres and that of living polymers was justified by MC simulations.[13]

TABLE 2: Transition Temperature for Nanocube with <100> Dipoles with Various Volume Fraction, Cube Size, and Dipole Strengths

ϕ	σ	μ	T_p	T_p^*
0.1	1.75	4.0	0.42	0.141
0.1	3.0	4.0	0.082	0.138
0.1	1.75	8.0	1.66	0.139
0.01	1.75	4.0	0.38	0.127
0.2	1.75	4.0	0.49	0.164

Next, we simulate nanocubes with <100> dipoles with varying volume fraction, cube size, and dipole strength. Table 2 lists parameters examined in this work. Under all these conditions, we find that the nanocubes self-assemble into straight wires as shown in Figure 2a. The T_p temperatures identified under these conditions are listed also in Table 2. The close proximity of reduced transition temperatures T_p^* in the first three rows of Table 2 implies that cube size and dipole strength do not affect the transition temperature under these conditions. Conversely, the last two rows in Table 2 show that the transition temperature increases from 0.38 to 0.49 when volume fraction increases from 0.01 to 0.2. The transition temperature increases with higher volume fractions, as expected from phase diagrams of other self-assembled systems.

3.2. Effect of Face−Face Attraction on Self-Assembly of Nanocubes with <100> Dipoles. Some applications of nanoparticle-assembled materials demand complex 2D and 3D structures. One of the possible strategies to assemble nanowires into structures of higher dimensions is to introduce face−face attractions between nanocubes. Such face−face attraction can arise in experiments by van der Waals interactions between nanocubes, or via hydrophobic interactions between stabilizers on nanocube surfaces. Here we examine the effect of face−face attractions on the self-assembled morphologies and the phase behavior of nanocubes with <100> dipoles. Three different attraction strengths ($\epsilon = 4$, 8, and 16) are studied here.

With $\epsilon = 4$, we find the nanocubes self-assemble into straight, rigid nanowires at $\phi = 0.1$ and $T = 0.38$, like those in Figure 2a. The potential energy plots for the cooling and heating processes (Figure 3b) also suggest a continuous, "equilibrium polymerization" type of transition as discussed in Section 3.1. However, the "polymerization" temperature T_p increases from 0.42 to 0.535 with the presence of face−face attractions. This is because such attractions facilitate the face-to-face alignment of nanocubes, allowing the polymerization transition to develop at higher temperatures.

With $\epsilon = 8$, we find the nanocubes self-assemble into stacked wires (Figure 2b) at $\phi = 0.1$ and $T = 0.815$, suggesting that such attractions are now strong enough to bring two neighboring wires together and coerce them into stacked configurations. Further increasing the face−face attraction to $\epsilon = 16$ results in sheet-like structures at $\phi = 0.1$ and $T = 1.34$ (Figure 2c), as the even stronger attractions encourage more strongly face-to-face alignment, leading to further close packing of the nanocubes.

3.3. Self-Assembly of Nanocubes with <110> Dipoles. As listed in Table 1, the <110> direction is another highly probable dipole direction besides the <100> dipole direction. Here we simulate nanocubes with <110> direction (model shown in Figure 1b) to examine the effect of dipole direction on the self-assembled morphologies.

Figure 2d shows a simulation snapshot of 100 nanocubes with a <110> dipole direction and no face−face attraction at $\phi = 0.2$ and $T = 0.24$. With <110> dipoles, the nanocubes self-assemble into sheets instead of the wires formed by <100> dipoles. As shown in Figure 2e, the dipole directions are parallel

within each sheet and antiparallel between neighboring sheets. Such dipole arrangements suggest that the minimization of dipole interactions, coupled with the unique geometry of cubes, dictates the assembled morphology. Specifically, the head-to-tail alignment of dipoles within each sheet minimizes the dipole−dipole interaction energy while preserving the face-to-face close packing of nanocubes. The antiparallel alignment of neighboring sheets introduces attractions between the nearest pair of dipoles between the two sheets (1 and 2 in Figure 2e) and repulsions between the second-nearest dipole pairs (1 and 3 in Figure 2e). The balance between the attractions and the repulsions determines the distance between the sheets. We note that the two sheets in the simulation snapshot are simultaneously formed from a disordered, random initial configuration. The orientation and distance between the two sheets are stable over the extended simulation time (600 million MCS). We note that all runs at this state point cooled from random initial conditions spontaneously form pairs of antiparallel sheets, suggesting that this is at least one stable structure at this state point. We do not observe any pairs of sheets for which the dipoles in the two sheets are at an angle other than 180 degrees. However, we cannot rule out the possibility that with certain orientation the two sheets could exhibit attractive overall interactions and aggregate into stacked sheets or even 3D crystals. Future simulations could investigate the impact of sheet orientations on their interactions and resulting structures. Figure 3c shows the potential energy versus temperature plots for cooling and heating processes. The hysteresis and discontinuity in potential energy suggests a first-order phase transition.

We note that such sheet structures are not reported in the experiment of Cho et al.[10] This is probably because of the possible mutual conversion between <110> and <100> dipoles in PbSe nanocubes. During the one-pot growth-and-assembly process in experiment, Se atoms can readily precipitate on Pb-terminated {111} corners and convert them into Se-terminated corners. Se-terminiated corners can also be converted into Pb-terminated corners with the precipitation of Pb atoms. Therefore, the distribution of polar {111} corners and the resulting dipole moments in PbSe nanocubes may change under experimental conditions. As predicted by our simulations, the wires formed from nanocubes with <100> dipoles are formed at a higher temperature than the sheets formed from nanocubes with <110> dipoles. With the cooling temperature profile employed by Cho et al., the first assembled wires can facilitate the conversion of a <110> dipole into a <100> dipole by promoting the energetically favored head-to-tail alignment between the newly converted <100> dipoles and the <100> dipoles in the existing wires. The absence of sheets also could be induced by net charges on the polar {111} corners. While it is easy to accommodate two adjacent charged corners from two neighboring cubes in wire structures by an alternating arrangement of positive and negative charges on cube corners, it is very difficult to closely pack four-charged corners from four-neighboring cubes on each lattice site in sheets, due to the substantial energy penalty of bringing more than two point charges in close proximity. Thus, the sheet structures predicted from our model should apply to nanocubes that have no point charges at the corners but have strong, permanent dipole moments in the cube cores, such as nanoparticles with anisotropic crystal structures.[27]

3.4. Mixture of Nanocubes with Different Dipole Strengths and Directions. Our computer simulations allow us to systematically regulate the composition of the system to investigate heterogeneous mixtures of dipole strengths and directions. As shown in Table 1, there are two possible dipole strengths for the <100> dipole direction with a ratio of 2:1. We simulate a mixture of ten cubes with dipole strength $\mu = 8$ and 40 cubes with strength $\mu = 4$, all with dipole direction <100>. Again, these nanocubes self-assemble into straight wires as in Figure 2a. The potential energy plots of the cooling and heating processes are shown in Figure 3d. Similar to Figure 3a,b, there is no discontinuity or hysteresis in the plots. The shape of the potential energy curve suggests that there are two independent equilibrium polymerization transitions, one for the $\mu = 8$ cubes at $T_{p1} = 1.44$, the other for the $\mu = 4$ cubes at $T_{p2} = 0.43$. The transition temperature for the $\mu = 8$ cubes is actually lower than the $T_p = 1.66$ listed for such cubes in Table 2. This is because the effective volume fraction of the $\mu = 8$ cubes in the mixed system is actually less than 0.1, and T_p decreases with lower volume fractions, as discussed in Section 3.1. The transition temperature for the $\mu = 4$ cubes is slightly higher than that ($T_p = 0.42$) listed for such cubes in Table 2, even though the effective volume fraction for the $\mu = 4$ cubes in the mixed system is slightly less than 0.1. This difference can be explained by the "catalytic" effect of the preassembled wires from the $\mu = 8$ cubes, as these wires function as "nucleation seeds" to facilitate the assembling of $\mu = 4$ cubes in the temperature range between T_{p1} and T_{p2}. Experimental studies of transition temperatures for mixed dipoles have not been reported, and thus our findings are presented here as a prediction.

Next, we simulate a system of mixed dipole directions and strengths in which 34 nanocubes have <100> dipoles of strength $\mu = 4$ and 16 nanocubes have <110> dipoles of strength $\mu = 5.66$. Figure 2f shows an example of a rectangular ring found in our simulations. This is similar to the nanorings observed in experiment.[10] Our simulation also confirms that, as in the schematic model proposed in Figure 9a of ref 10, the <100> cubes form the long edges of the rectangular rings and the <110> cubes connect the <100> edges into rings. We notice that there is four-way packing of cubes at the corners of the rectangular ring in our simulation snapshot, which is not observed in experiment. This difference also may be caused by the presence of corner point charges and the resulting less closely packed arrangement of nanocubes in experiment.

4. Conclusion

In this paper, we investigated the dipole induced self-assemblies of nanocubes with and without attractive face−face interactions. We showed that the well-known head-to-tail alignment of dipoles, coupled with the direction of the dipole within the cube, produces diverse assembled morphologies. In particular, nanocubes with <100> dipoles form straight wires, agreeing with the morphologies observed in the experiment conducted by Cho et al.[10] Nanocubes with <110> dipoles are predicted to form sheets in our model. The possible net charges on PbSe nanocubes are a likely reason for the absence of such sheets in the experimental studies. The potential energy versus temperature plots from our simulations suggest that the wires are formed by a continuous transition similar to equilibrium polymerization, as in dipolar fluids. The reduced transition temperature is independent of cube size and dipole strength, but increases with volume fraction. Our simulations on nanocube systems of mixed dipole directions successfully reproduce the nanorings observed in the experiment and confirm the proposed schematic model in ref 10. We also examined the effect of face−face attractions and predicted that strong attractions will force nanocubes into stacked wires and sheetlike configurations, whereas weak attraction will not alter the assembled wire structures but only increase the transition temperature.

Our results demonstrate that nanocubes with dipoles are promising candidates for bottom-up materials design, as one can control the assembled morphologies and the phase behavior by manipulating dipole directions, dipole strengths, and face−face attraction. The simulation code developed for this study can be utilized to investigate the self-assemblies of all smooth, convex polyhedra with directional dipole interactions, which could lead to a rich variety of assembled morphologies and reveal new opportunities in nanomaterials design.

As discussed in Section 3, the few differences between our simulation results and the experiments are likely due to the conversion between dipole directions under experimental conditions and the possible presence of point charges on PbSe nanocube corners. Recently, Tang et al. have demonstrated that both dipolar and Coulombic interactions are essential for CdTe nanoparticles to self-assemble into sheets.[20] Our model may be expanded to include the effect of dynamic dipole moments and point charges to study their impact on nanocube self-assemblies in future work.

Acknowledgment. Financial support for this work was provided by the National Science Foundation under Grant No. DMR-0103399 and by the Department of Energy under Grant No. DE-FG02-02ER46000. We thank the University of Michigan Center for Advanced Computing for computer cluster support.

References and Notes

(1) Whitesides, G. M.; Grzybowski, B. *Science* **2002**, *295*, 2418.
(2) Glotzer, S. C.; Solomon, M. J.; Kotov, N. A. *AIChE J.* **2004**, *50*, 2978.
(3) Rogach, A. L.; Talapin, D. V.; Shevchenko, E. V.; Kornowski, A.; Haase, M.; Weller, H. *Adv. Funct. Mater.* **2002**, *12*, 653.
(4) Yamamuro, S.; Sumiyama, K. *Chem. Phys. Letters* **2006**, *418*, 166.
(5) Pileni, M. P. *J. Phys. Chem. B* **2001**, *105*, 3358.
(6) Tang, Z. Y.; Kotov, N. A. *Adv. Mater.* **2005**, *17*, 951.
(7) Tang, Z. Y.; Kotov, N. A.; Giersig, M. *Science* **2002**, *297*, 237.
(8) Tang, Z. Y.; Ozturk, B.; Wang, Y.; Kotov, N. A. *J. Phys. Chem. B* **2004**, *108*, 6927.
(9) Giersig, M.; Pastoriza-Santos, I.; Liz-Marzán, L. M. *J. Mater. Chem.* **2004**, *14*, 607.
(10) Cho, K. S.; Talapin, D. V.; Gaschler, W.; Murray, C. B. *J. Am. Chem. Soc.* **2005**, *127*, 7140.
(11) Teixeira, P. I. C.; Tavares, J. M.; da Gama, M. M. T. *J. Phys.: Condens. Matter* **2000**, *12*, R411.
(12) Weis, J. J.; Levesque, D. *Phys. Rev. Lett.* **1993**, *71*, 2729.
(13) Tavares, J. M.; Weis, J. J.; da Gama, M. M. T. *Phys. Rev. E* **1999**, *59*, 4388.
(14) Stevens, M. J.; Grest, G. S. *Phys. Rev. E* **1995**, *51*, 5962.
(15) Clarke, A. S.; Patey, G. N. *J. Chem. Phys.* **1994**, *100*, 2213.
(16) McGrother, S. C.; Jackson, G. *Phys. Rev. Lett.* **1996**, *76*, 4183.
(17) van Leeuwen, M. E.; Smit, B. *Phys. Rev. Lett.* **1993**, *71*, 3991.
(18) McGrother, S. C.; Gil-Villegas, A.; Jackson, G. *Mol. Phys.* **1998**, *95*, 657.
(19) Teixeira, P. I. C.; Osipov, M. A.; da Gama, M. M. T. *Physical Review E* **1998**, *57*, 1752.
(20) Tang, Z. Y.; Zhang, Z. L.; Wang, Y.; Glotzer, S. C.; Kotov, N. *Science* **2006**, *314*, 274.
(21) de Leeuw, S. W.; Perram, J. W.; Smith, E. R. *Proc. R. Soc. London, Ser. A* **1980**, *373*, 27.
(22) Adams, D. J.; Adams, E. M. *Mol. Phys.* **1981**, *42*, 907.
(23) Van Workum, K.; Douglas, J. F. *Phys. Rev. E* **2005**, *71*.
(24) Allen, M. P.; Tildesley, D. J. *Computer Simulation of Liquids*; Clarendon Press: Oxford, 1987.
(25) Schneider, P.; Eberly, D. H. *Geometric Tools for Computer Graphics*; Morgan Kaufmann: San Francisco, CA, 2003.
(26) John, B. S.; Escobedo, F. A. *J. Phys. Chem. B* **2005**, *109*, 23008.
(27) Shim, M.; Guyot-Sionnest, P. *J. Chem. Phys.* **1999**, *111*, 6955.